Published in final edited form as:
J Immunol. 2013 May 1; 190(9): 4640–4649. doi:10.4049/jimmunol.1202312.

Role of Fatty-acid Synthesis in Dendritic Cell Generation and Function

Adeel Rehman[1,*], **Keith C. Hemmert**[2,*], **Atsuo Ochi**[1], **Mohsin Jamal**[1], **Justin R. Henning**[1], **Rocky Barilla**[1], **Juan P. Quesada**[1], **Constantinos P. Zambirinis**[1], **Kerry Tang**[1], **Melvin Ego-Osuala**[1], **Raghavendra S. Rao**[1], **Stephanie Greco**[1], **Michael Deutsch**[1], **Suchithra Narayan**[1], **H. Leon Pachter**[1], **Christopher S. Graffeo**[2], **Devrim Acehan**[2], and **George Miller**[1]

[1]S. Arthur Localio Laboratory, Department of Surgery, New York University School of Medicine, 550 First Avenue, New York, NY 10016

[2]Department of Cell Biology, New York University School of Medicine, 550 First Avenue, New York, NY 10016

Abstract

Dendritic cells (DC) are professional antigen presenting cells that regulate innate and adaptive immunity. The role of fatty-acid synthesis in DC development and function is uncertain. We found that blockade of fatty-acid synthesis markedly decreases dendropoiesis in the liver and in primary and secondary lymphoid organs in mice. Human DC development from PBMC precursors was also diminished by blockade of fatty-acid synthesis. This was associated with higher rates of apoptosis in precursor cells and increased expression of Cleaved Caspase 3 and BCL-xL, and down-regulation of Cyclin B1. Further, blockade of fatty-acid synthesis decreased DC expression of MHCII, ICAM-1, B7-1, B7-2 but increased their production of selected pro-inflammatory cytokines including IL-12 and MCP-1. Accordingly, inhibition of fatty-acid synthesis enhanced DC capacityto activate allogeneic as well as antigen-restricted $CD4^+$ and $CD8^+$ T cells and induce CTL responses. Further, blockade of fatty-acid synthesis increased DC expression of Notch ligands and enhanced their ability to activate NK cell immune-phenotype and IFN-γ production. Since endoplasmic reticular (ER)-stress can augment the immunogenic function of APC, we postulated that this may account for the higher DC immunogenicity. We found that inhibition of fatty-acid synthesis resulted in elevated expression of numerous markers of ER stress in humans and mice and was associated with increased MAP kinase and Akt signaling. Further, lowering ER-stress by 4-phenylbutyrate mitigated the enhanced immune-stimulation associated with fatty-acid synthesis blockade. Our findings elucidate the role of fatty-acid synthesis in DC development and function and have implications to the design of DC vaccines for immunotherapy.

Keywords

Fatty-acid synthesis; Bone marrow dendritic cells; ER stress; T cells; NK cells

Introduction

Dendritic cells (DC) have emerged over the past two decades as the most specialized professional antigen presenting cells which initiate adaptive and innate immune responses

Contact Information: George Miller, MD, Departments of Surgery and Cell Biology, New York University School of Medicine, Medical Science Building 601, 550 First Avenue, New York, NY 10016, Tel: (212) 263-1479, Fax: (212) 263-6840, george.miller@nyumc.org.

*AR and KCH contributed equally toward this work

(1). As a consequence, DC have an important role in immune surveillance against developing cancer or invading pathogens and have potential to serve a vehicles for immunotherapy. Hence, elucidating the cellular biochemistry of DC has implications both for understanding immunity and for the design of immunotherapy regimens.

Fatty-acid synthesis is an essential element of cellular metabolism. However, its role in DC development and function is uncertain. A study by Zeyda et al. (2) investigated the effects of exogenous administration of polyunsaturated fatty-acids (PUFA) to DC and found that PUFA blocks DC immunogenic function independent of NF-κB activation. In particular, DC capacity for T cell activation was markedly inhibited in DC treated with PUFA. Similarly, a more recent report by Herber et al. (3) found that DC acquire exogenous lipids within the tumor microenvironment in both mice and humans which renders them poorly functional, accounting for their inability to generate a potent anti-tumor immune response. The diminished DC immunogenicity facilitates the cancer's capacity to evade immune recognition. Nevertheless, whereas exogenous fatty-acids - either directly administered or accumulated in tumor bearing hosts - appear to lessen the immunogenic potential of DC, the role of endogenous fatty-acid synthesis on dendropoiesis in vitro and in vivo and on DC functional properties is uncertain. In this study, we found that blocking fatty-acid synthesis using either inhibitors of Acetyl CoA carboxylase or fatty-acid synthase diminished dendropoiesis from bone marrow or PBMC precursors. However, surprisingly, inhibition of fatty-acid synthesis upregulated DC expression of Toll-like receptors and markedly augmented DC capacity to stimulate antigen restricted $CD4^+$ and $CD8^+$ T cells, induce CTL, and activate innate immune effector cells. Our mechanistic studies revealed that blockade of fatty-acid synthesis enhances MAP Kinase, PI3Kinase/Akt, and Notch signaling in DC and leads to higher endoplasmic reticulum (ER) stress. These findings suggest an important role for fatty-acids synthesis in modulating basic DC biology and have implications for the design of more effective immunotherapy regimens.

Methods

Animals

Male C57BL/6 (H-$2k^b$), BALB/c (H-$2k^d$), OT-I (B6.Cg-RAG2tm1Fwa-TgN), and OT-II (B6.Cg-RAG2tm1Alt-TgN) mice were purchased from Taconic (Germantown, NY, USA). Age-matched 6–8 week old mice were used in experiments. Animals were housed in a clean vivarium and fed standard mouse chow. In selected experiments, mice were injected thrice weekly for four weeks with saline or C75 (250μg, i.p.; Sigma-Aldrich, St. Louis, MO), an inhibitor of fatty-acid synthase. Animal procedures were approved by the New York University School of Medicine Institutional Animal Care and Use Committee.

Murine Bone Marrow DC and Human moDC Generation

Bone marrow derived DC (BMDC) were generated as described (4). Briefly, bone marrow aspirates were cultured for eight days in complete RPMI (RPMI 1640 with 10% heat inactivated FBS, 2 mML-glutamine, and 0.05mM 2-ME) supplemented with GM-CSF (20 ng/ml). To generate human moDC, leukocyte-enriched buffy coats were obtained from the New York Blood Center. PBMCs were separated by density gradient centrifugation on Ficoll-Hypaque (GE Healthcare, Piscataway, NJ). Cells were cultured for 5–7 days in complete RPMI supplemented 10% human serum, 800 U/mL GM-CSF, and 1000 U/mL IL-4 (R&D Systems, Minneapolis, MN). In selected experiments, Acetyl CoA carboxylase was inhibited in murine BMDC or human moDC cellular suspensions using TOFA (5μg/dl; Cayman Chemical, Ann Arbor, Michigan) beginning on day 2 of culture (5–7). In selected experiments a lower dose of TOFA was used (1μg/dl). Ethanol (0.5%) was used a solvent

for TOFA. In additional experiments, staurosporine (10μM) was employed to induce DC apoptosis (8, 9).

Leukocyte Isolation from Liver and Spleen

Murine hepatic non-parencymal cells (NPC) were isolated as described (10). Briefly, the portal vein was infused with Collagenase IV (Sigma-Aldrich) followed by hepatectomy and mechanical digestion. Hepatocytes were excluded by serial low speed (300 RPM) centrifugation. NPC were further enriched over an Optiprep (Sigma-Aldrich) gradient. Splenocytes were isolated by manual disruption of whole spleen. In selected experiments, splenic T cells and NK cells were purified by FACS or using anti-CD90, anti-CD4, anti-CD8, or anti-DX5 immunomagnetic beads, respectively, and passage through positive selection columns (Miltenyi, Bergisch-Gladbach, Germany).

Flow Cytometry and Cytokine Analysis

Flow cytometry was performed using the FACS Caliber (Beckton-Dickinson, Franklin Lakes, NJ) after incubating 5×10^5 cells/tubewith 1μg of anti-FcγRIII/II antibody (2.4G2, Fc block; Monoclonal Antibody Core, Sloan-Kettering Institute, New York, NY) and then labeling with1 μg of a fluorescently-conjugated mAb against MHC II ($I\text{-}A^b$), CD4 (RM4-5) CD8α (53–6.7), CD11b (M1/70), CD11c (HL3), CD19 (1D3), CD25 (3C7), CD40 (HM40-3), CD45 (30-F11), CD54 (YN1/1.7.4), B7-1 (16-10A1), B7-2 (GL1), Foxp3 (FJK-16s; all eBioscience, San Diego, CA), CD3ε (145-2C11; BioLegend, San Diego, CA), and TLR2 (T2.5) (Imgenex, San Diego, CA). Alternatively, cells were labeled with unconjugated antibodies against Jagged-1 (Santa Cruz Biotechnology, Santa Cruz, CA), TLR4, TLR7 and TLR9 (all Imgenex) and subsequently stained with fluorescently labeled secondary antibodies. Human moDC were tested using mAbs directed against HLA-DR and CD11c (BD Biosciences, Franklin Lakes, NJ). For cytokine analysis, cell suspensions were cultured in complete RPMI at a concentration of 1×10^6 cells/ml for 24h before supernatant harvest and analysis either using either a cytometric bead array (BD Biosciences) or the Milliplex Immunoassay (Millipore, Billerica, MA).

In Vitro T cell Assays and CTL Assays

For $CD4^+$ or $CD8^+$ T cell proliferation assays, BMDC were pulsed with the appropriate Ova peptide (10μg/ml, Abcam, Cambridge, Massachusetts) for 90 minutes before washing and plating, respectively, with $CD4^+$OT-II TCR-transgenic T cells (1×10^5) specific for $Ova_{323–339}$ peptide or$CD8^+$OT-I TCR-transgenic T cells specific for $Ova_{257–264}$ peptide for 72h in 96 well plates as described (10). In selected experiments, non-peptide-pulsed DC were used to stimulate allogeneic BALB/c T cells in a mixed leukocyte reaction (MLR) as described (10). For cross-presentation experiments, DC were loaded with Ovalbumin (1mg/ml, Sigma-Aldrich) and used to stimulate OT-I T cells as described (10). For the last 24h, 1μCi [^{3}H]-Thymidine was added to wells and proliferation measured using a MicroBeta counter (Perkin Elmer, Waltham, Massachusetts). Alternatively, T cell activation was assessed by measuring Th1, Th2, and Th17 cytokine production using a cytometric bead array or by examination of T cell surface phenotype. In selected experiments, soluble inhibitors of PI3 Kinase (50uM, LY294002) and MAP Kinase (100uM, PD98059; both Invivogen, San Diego, CA) signaling were employed. To assess BMDC induction of regulatory T cells, DC were cultured with equal numbers of splenocytes before determination of $CD4^+$ T cell co-expression of CD25 and FoxP3 at 96 hours. In some experiments, BMDC were incubated overnight with the chemical chaperone 4-phenylbutyrate (10mM, Sigma-Aldrich) before washing, peptide loading, and co-culture with T cells. To determine the ability of DC to produce a CTL response in vivo, naïve mice were immunized i.p. twice at weekly intervals with $DC.Ova_{257–264}$ (3×10^5) or mock immunized. One week later, splenocytes were harvested from immunized mice, restimulated

in vitro with $Ova_{257–264}$, and cell culture supernatant assayed for IFN-γ and IL-10 as described (4).

NK Cell Assays

DC-NK cell co-cultures were performed as described with slight modifications (4). Briefly, splenic NK cells (1×10^5) were plated with BMDC (1×10^5) in a 1:1 ratio in 96-well plates for 24h. IFN-γ was measured in cell culture supernatant using a cytometric bead assay (BD Biosciences). In addition, NK cell expression of CD25 was analyzed by flow cytometry.

Antigen Capture Assays

To assess DC capacity for antigenuptake, BMDC were incubated with FITC-Dextran, FITC-Albumin, or FITC-Mannose Albumin (1 mg/ml; all Sigma-Aldrich) at 37°C forvarious time intervals. Antigen uptake was determined by flow cytometry. For in vivo antigen uptake, control or C75-treated mice were injected i.p. with 1mg of FITC-Albumin. Mice were then sacrificed at 30 minutes and splenic DC fluorescence determined by flow cytometry.

Microscopy & Lipid Analysis

For light and fluorescent microscopic analysis, cells were spun onto slides and stained with H&E, Giemsa, HCS LipidTOX Red specific for neutral lipids, and HCS LipidTOX Green specific for phospholipids (Invitrogen, Grand Island, NY). Light microscopic images were captured using an Axiovert 40 microscope (Zeiss, Thornwood, NY). Fluorescent images were captured on an Axiovert 200M (Zeiss). Cells were also tested by flow cytometry using BODIPY (Invitrogen) as described (11). For electron microscopic analysis, BMDC suspensions were first incubated with 4% formaldehyde and 2% glutaraldehyde (GA) in 0.1M pH 7.5 Pipes buffer (PB) for 30 minutes at room temperature. Cells were further fixed with 4% GA and 0.4% tannic acid in PB for 30 minutes followed by 2% osmium tetroxide in PB for 1h. The samples were then counter-stained with 2% uranylacetate (UrAc) for 12h at 4°C before exchanging the solution with ethanol. Samples were then infused with epoxy resin and polymerized at 60°C. The sample blocks were sectioned to a thickness of 50–70 μm, collected on electron microscope grids and stained with UrAc and Sato Lead Stain. The samples were then imaged using a Philips CM12 microscope (Philips, Eindhoven, Netherlands). For each section, the cellular, nuclear, and cytosolic areas were estimated by assuming the cell and nucleus sections are ellipses and measuring the long and short axes. To measure the rate of intracellular fatty-acid synthesis in BMDC, C-14 labeled acetate was added to BMDC cultures (2μCi/well) for 6 hours. More than 40 cells from each treatment group were analyzed. Intracellular lipids were isolated by the Folsch extraction method and C-14 uptake was determined by scintigraphy as described (11).

Western Blotting

Western blotting was performed as described (11, 12). Briefly, BMDC were homogenized in RIPA buffer and proteins were separated from larger fragments by centrifugation at 14000 × g. Samples were equiloaded onto 10 % polyacrylamide gels (NuPage, Invitrogen), electrophoresed at 200 V, electrotransferred to PVDF membranes, and probed with monoclonal antibodies to GRP-78, eIF2α, p- eIF2α, XBP-1, PPAR-γ, Caspase 3, BCL-xL, Cyclin B1, Jagged-1, Delta-4, Akt, pAkt, Erk1, pErk1, NF-κB, pNF-κB, PTEN, p38MAP Kinase, p-p38MAP Kinase, p70S6 kinase, and β-actin (all Santa Cruz Biotechnology). Blots were developed by ECL (Thermo Scientific, Asheville, NC).

Statistics

Statistics were calculated using GraphPad Prism V5.00 (GraphPad Software, San Diego, CA). Data is presented as mean +/− standard error of the mean. Statistical significance ($p<0.05$) was determined using the Student's *t* test and the log-rank test.

Results

Blockade of fatty-acid synthesis inhibits dendropoiesis

To determine whether blockade of fatty-acid synthesis in vivo affects dendropoiesis in lymphoid and non-lymphoid organs, mice were serially administered C75, an inhibitor of fatty-acid synthase (13, 14), and the number of $CD11c^+$ cells was measured in the bone marrow, spleen, and liver. Treatment for 4 weeks resulted in an 80% reduction in the fraction and total number of $CD11c^+$ cells in the liver (Figure 1a, b) and an approximate 20% reduction in the spleen and bone marrow (Figure 1b). Other cell types, including B cells, T cells, neutrophils, and macrophages were not affected (Figure 1c).

To investigate the effects of inhibition of fatty-acid synthesis on DC generation in vitro from bone marrow precursors, we isolated bone marrow cells and cultured them in GM-CSF supplemented media for 8 days to drive dendropoiesis, as described (4). In parallel, for the duration of in vitro culture, bone marrow cells were co-incubated with TOFA, which inhibits acetyl CoA corboxylase (15, 16). The number of non-viable PI^+ cells was increased on day 8 of culture (Figure 1d) as well as at earlier time points (not shown) in cellular suspensions incubated with TOFA. Further, there was increased expression of cleaved caspase-3 and BCL-xL in TOFA-treated BMDC (T-BMDC), consistent with increased rates of apoptosis (Figure 1e). Accordingly, Cyclin B1, an anti-apoptotic gene was down-regulated in T-BMDC (Figure 1e). The total number and fraction of $CD11c^+$ cells produced per mouse femur (Figure 1f) and BMDC cellular proliferation (Figure 1g) were also lower in TOFA-treated bone marrow cultures. Generation of human moDC was similarly hindered by TOFA (Figure 1h). Furthermore, serial in vivo administration of C75 resulted in less efficient generation of BMDC after bone marrow harvest (Supplemental Figure 1a). Taken together, these data show that blockade of fatty acid synthesis inhibits dendropoiesis in vitro and in vivo and in both mice and humans.

Inhibition of fatty-acid synthesis alters DC morphology and surface phenotype

As anticipated, bone marrow-derived cells grown in TOFA exhibited a decreased rate of fatty-acid synthesis (Figure 2a). Accordingly, on both electron microscopy and light microscopy, T-BMDC exhibited decreased vacuolization and numbers of lipid droplets (Figure 2b, c and Supplemental Figure 1b). Similarly, HCS LipidTOX Red staining revealed a substantial reduction in total neutral lipids (Figure 2d and Supplemental Figure 1c) and HCS LipidTOX Green staining revealed decreased phospholipid levels in T-BMDC (Figure 2e and Supplemental Figure 1d). Further, T-BMDC had diminished staining for BODIPY which binds total neutral lipids (Supplemental Figure 1e).

Since we found that inhibition of fatty-acid synthesis prevents dendropoiesis, we postulated that it may also affect BMDC maturation. To test this, bone marrow derived $CD11c^+$ cells were analyzed for expression of MHCII, co-stimulatory, and adhesion molecules. As anticipated, T-BMDC exhibited decreased expression of MHCII, ICAM-1, B7-1, and B7-2 (Figure 2f). However, CD40 and CD11b were consistantly upregulated in BMDC grown in TOFA (Figure 2f). Similar phenotypic differences between T-BMDC and controls were seen when gated exclusively on $CD11c^+MHCII^+$ cells (not shown). Surprisingly, despite a diminished maturational phenotype, blockade of fatty-acid synthesis upregulated DC surface expression of TLR2 and TLR4 and intra-cellular expression TLR7 and TLR9 (Figure 2g).

Conversely, in contrast to the effects of TOFA, staurosporine, which also induced BMDC apoptosis (Supplemental Figure 2a), upregulated MHCII expression on BMDC (Supplemental Figure 2b) and did not increase BMDC TLR expression (Supplemental Figure 2c), suggesting that effects of TOFA are specific to fatty acid synthesis inhibition.

TOFA increases endoplasmic reticulum stress, PPAR-γ expression, and cytokine production in BMDC

Endoplasmic reticulum (ER) stress can have marked affects on the immune-stimulatory capacity of antigen presenting cells (17–19). Since inhibition of fatty-acid synthesis induces ER stress in neoplastic cells (20), we postulated that TOFA-grown BMDC would exhibit high ER stress. In consort with our hypothesis, we found that GRP-78, eIF2α, p-eIF2α, and XBP-1, all markers of ER stress (21), were more highly expressed in T-BMDC compared with controls (Figure 3a). Human moDC generated in TOFA also expressed markedly elevated p-eIF2α (Figure 3b). Higher PPAR-γ expression has been linked to increased ER stress and is associated with enhanced DC capacity to present antigen (22–25). Accordingly, we found substantial upregulation of PPAR-γ expression in murine T-BMDC at both the protein (Figure 3c) and mRNA levels (Figure 3d). TOFA-treated human moDC also expressed higher PPAR-γ (Figure 3e).

The respective roles ER stress or endogenous fatty-acid synthesis on DC production of immune-modulatory cytokines and chemokines are uncertain. Since DC regulate immunity by production of soluble inflammatory mediators, we tested T-BMDC cytokine and chemokine production. BMDC production of an array of inflammatory mediators including IL-1α, IL-1β, IL-6, IL-10, IL-12, IFN-γ, IP-10, KC, LIF, MCP-1, M-CSF, MIG, MIP-2, and G-CSF were higher in T-BMDC compared with controls (Figure 3f, g). However, the CC chemokines MIP-1α, MIP-1β, and RANTES were expressed at markedly lower levels in T-BMDC (Figure 3h). Lower dose TOFA (1mg/dl) also increased BMDC cytokine production, however, 0.5% ethanol alone had no effect nor did staurosporine (Figure 3i).

Blockade of fatty-acid synthesis enhances DC capacity for antigen capture

Antigen uptake is a primary function of DC and a critical consideration in constructing DC vaccines for cancer immunotherapy (26, 27). To determine the role of fatty-acid synthesis in DC capacity to capture antigen, BMDC were grown alone or in media supplemented with TOFA, as above. Consistent with their relative immaturity, T-BMDC exhibited enhanced ability to capture antigen via generalized macropinocytosis (Figure 4a) or using specialized mannose receptors (Figure 4b, c). Similarly, serial treatment of mice with C75 resulted in markedly enhanced spleen DC capacity to capture antigen in vivo (Figure 4d). Low dose TOFA was similarly effective at enhancing DC capacity for antigen capture as high dose TOFA (Supplemental Figure 3a). Conversely, Ethanol or staurosporine did not enhance DC ability to capture soluble antigen (Supplemental Figure 3b). These data imply that blockade of fatty-acid synthesis enhances DC capacity for antigen capture in multiple contexts.

Inhibition of fatty-acid synthesis enhances BMDC capacity to activate allogeneic and antigen-restricted $CD4^+$ and $CD8^+$ T cells

Since blockade of fatty-acid synthesis augments BMDC ER stress and increases their production of inflammatory mediators, we postulated it would enhance their immune stimulatory function. In consort with our hypothesis, T-BMDC induced higher proliferation of allogeneic T cells in an MLR compared with controls (Figure 5a). To determine the effect of inhibiting fatty-acid synthesis on DC capacity to stimulate antigen-restricted $CD4^+$ T cell, control or T-BMDC were loaded with $Ova_{323–339}$ and then co-cultured in various concentrations with $CD4^+$ OT-II T cells. Peptide-pulsed BMDC grown in TOFA induced more vigorous proliferation of antigen-restricted $CD4^+$ T cells (Figure 5b) and induced

higher $CD4^+$ T cell production of Th1 and Th17 cytokines (Figure 5c) compared with peptide-pulsed control BMDC stimulators. Conversely, Th2 cytokines were uniformly expressed at low levels after stimulating OT-II cells using either BMDC or T-BMDC. There was similarly no significant difference between control and T-BMDC in their propensity to generate $CD4^+CD25^+Foxp3^+$ regulatory T cells in co-culture experiments (Figure 5d). Low dose TOFA was also effective at enhancing DC capacity for antigen presentation. Conversely, staurosporine diminished DC capacity for T cell stimulation (Supplemental Figure 3c).

To explore whether the increased immunogenicity of TOFA-treated BMDC extends to their interactions with $CD8^+$ T cells, we loaded BMDC populations with $Ova_{257–264}$ before co-culture with $CD8^+$ OT-I T cells. Peptide-pulsed T-BMDC induced approximately 3-fold elevated $CD8^+$ T cell proliferation (Figure 6a). In addition, BMDC grown in TOFA induced higher CD44 expression in antigen-restricted $CD8^+$ T cells (Figure 6b) and markedly increased $CD8^+$ T cell production of IFN-γ (Figure 6c) and TNF-α (Figure 6d) compared with peptide-pulsed control BMDC stimulators. Further, to determine the effect of blocking fatty-acid synthesis on DC capacity to cross-present antigen to $CD8^+$ T cells, control or T-BMDC were loaded with Ovalbumin and cultured at various concentrations with $CD8^+$ OT-I T cells. Again, T-BMDC induced enhanced cross presentation of Ovalbumin as evidenced by higher T cell proliferation (Figure 6e) and production of IFN-γ (Figure 6f).

T-BMDC induce high CTL in vivo

DC are largely reliant on their capacity to induce CTL in their effort to target invading pathogens or cancer cells (28). To determine the requirement for fatty-acid synthesis during DC generation on their ability to generate CTL in vivo, mice were immunized twice at weekly intervals with $Ova_{257–264}$ peptide-pulsed control BMDC or T-BMDC. Splenocytes were harvested from immunized mice one week after the second immunization and were restimulated in vitro with $Ova_{257–264}$ peptide. On day 5, CTL cultures were tested for production of IFN-γ and IL-10. Consistent with our previous findings, in vivo immunization using T-BMDC induced elevated production of IFN-γ in CTL supernatant (Figure 6g). Moreover, T-BMDC immunization resulted in decreased production of IL-10 - an inhibitory cytokine - in CTL cultures compared with immunization using peptide-pulsed control BMDC (Figure 6h). Taken together, these data suggest that blockade of fatty-acid synthesis is an attractive strategy to enhance DC capacity for induction of immunogenic CTL responses.

Blockade of fatty-acid synthesis enhances MAP Kinase and PI3 Kinase/Akt signaling in BMDC

Since DC immune-stimulatory capacity has been linked to the MAP Kinase, NF-κB, and PI3K/Akt signaling pathways (29), we tested the effect of inhibition of fatty-acid synthesis on the cellular activation of these pathways. Consistent with their enhanced $CD4^+$ and $CD8^+$ T cell stimulatory capacity, we found that T-BMDC expressed elevated levels of pErk-1, an activated MAP Kinase signaling intermediate (Supplemental Figure 4a). We also found that T-BMDC expressed elevated levels of pAkt as well as p70 S6 kinase, which acts downstream of PIP3, suggesting activation of the PI3 Kinase/Akt signaling pathway in BMDC in the context of fatty acid synthesis blockade (Supplemental Figure 4b). PTEN which negatively regulates the PI3 Kinase/Akt signaling was equally expressed in TOFA-treated and control BMDC (Supplemental Figure 4b). However, activated NF-κB intermediates were expressed at lower levels after TOFA treatment, which is consistent with their elevated intracellular ER stress (30) (Supplemental Figure 4c).

Enhanced T cell stimulatory capacity of TOFA-treated BMDC is contingent on their higher ER stress

Elevated ER stress has been linked to enhanced antigen presentation by APC (31). Since the chaperone 4-phenylbutyrate inhibits adipogenesis by modulating the unfolded protein response and decreasing ER stress (32), we postulated this may mitigate the increased immunogenicity of TOFA-treated BMDC. Accordingly, we found that the pre-incubation with 4-phenylbutyrate significantly reduced the $CD4^+$ and $CD8^+$ T cell stimulatory capacity of T-BMDC (Figure 7a, b). T cell activation by control BMDC was affected to a lesser extent by the chaperone. These data imply that the increased immunogenicity of T-BMDC may be related to their increased ER stress. Blockade of MAP Kinase or PI3K/Akt signaling did not mitigate the augmented capacity of T-BMDC to induce T cell proliferation (Figure 7c). However, MAP Kinase inhibition lessened T cell activation (Figure 7d). PI3 Kinase blockade had no effect (data not shown)

Blockade of fatty-acid synthesis enhances BMDC capacity to activate NK cells

We and others have demonstrated that BMDC are powerful activators of innate immune effector cells such as NK and NKT cells (33, 34). To examine the role of fatty-acid synthesis in BMDC capacity to activate NK cells, we co-cultured T-BMDC and controls with equal numbers of NK cells before NK cell harvest and measurement of their phenotypic activation and production of IFN-γ. T-BMDC induced elevated NK cell expression of CD25 (Figure 8a) and induced nearly 4-fold higher production of IFN-γ compared with control BMDC (Figure 8b). Since DC capacity to activate NK cells has recently been linked to their expression of Notch ligands (35), we tested whether blockade of Acetyl CoA corboxylase secondarily increases Notch ligand expression in BMDC. As postulated, T-BMDC expressed higher Jagged-1 and Delta-4 compared with control BMDC on analysis by Western blotting (Figure 8c) and flow cytometry (Figure 8d).

Discussion

Dendritic cells are a specialized population of antigen presenting cells that link innate and adaptive immunity (1). DC can influence immune responses by both direct interaction with effector cells, such as T cells and NK cells, and via production of a wide array of inflammatory mediators. In this study, we found that blockade of fatty-acid synthesis markedly inhibits DC development from bone marrow or PBMC precursors in mice and humans, respectively, and induces apoptosis in DC precursors, which is associated with elevated cellular expression of Cleaved Caspase 3, BCL-xL, and down-regulation of Cyclin B1. For our in vivo experiments, we employed C75 in lieu of TOFA as TOFA is highly toxic when administered systemically (7, 36). We found that in vivo blockade of fatty-acid synthesis hinders DC generation in peripheral tissues as well as primary and secondary lymphoid organs. Fatty-acid synthesis inhibition also has variable effects on DC surface phenotype including suppression of MHC II expression but increased CD40 expression. Further, T-BMDC express higher levels of selected MAP Kinase and PI3K/Akt signaling intermediates and produce markedly elevated levels of numerous cytokines and chemokines (37, 38). Interestingly, the CC chemokines MIP-1α, MIP-1β, and RANTES, which are purported to play a role in granulocytic lineage proliferation or differentiation (39), are suppressed by fatty-acid synthesis inhibition. Understanding the mechanistic regulation of BMDC cytokine and chomkine production by fatty acid synthesis requires more exact study; however, there are likely to be autocrine effects of specific cytokines on further BMDC production of additional inflammatory mediators. For example, Stober et al. reported that IL-12 can influence IFN-γ production by BMDC (40). Taken together, our data suggest that the capacity for fatty-acid synthesis is important for DC generation and expression of their distinct immune-phenotype.

The properties of DC generated in the context of fatty-acid synthesis blockade are relevant not only to understanding basic DC immuno-biology but also for the development of vaccines for immunotherapy. In particular, TOFA-treated DC exhibited increased capacity to activate $CD4^+$ and $CD8^+$ T cells and NK cells which can be exploited in the construction of DC cancer vaccines. T-BMDC induction of antigen-restricted $CD8^+$ T cells led to increased production of IFN- γ and TNF-α, and decreased production of IL-10. DC immunotherapy regimens in cancer and benign diseases have largely been of limited clinical efficacy because of the modest adaptive immune responses and CTLs induced (28, 41). Varied cytokine cocktails and methods of exogenous DC stimulation have been employed to bolster the host's antigen-restricted and innate immunogenic responses to DC vaccines (28); hence, our data suggest that inhibiting fatty-acid synthesis may be an attractive adjuvant in experimental immunotherapy.

The mechanism for the enhanced immune-stimulatory capacity of DC generated in the context of fatty-acid synthesis inhibition appears to be related in part to their elevated ER stress. ER stress is generated in response to an accumulation of unfolded or misfolded proteins in the lumen of the endoplasmic reticulum (42). ER stress attempts to restore normal cellular function by halting protein translation and activating signaling pathways leading to production of molecular chaperones that facilitate protein folding. This process has been found to be conserved among all mammalian species, and can result in cellular apoptosis if not resolved (43). There is an emerging role for ER stress in the function of antigen presenting cells. Goodall et al. reported that activation of ER stress, in combination with Toll-like receptor ligation, markedly enhances DC expression of selected cytokines (44). Additionally, Oh et al. recently reported that ER stress is a functional switch regulating M2 macrophage differentiation and phenotype including cellular cholesterol content (45). Our observations of elevated ER stress in TOFA-treated BMDC were made in both our murine and human models and were further adduced by higher DC expression of PPAR-γ after TOFA treatment. Further, our finding of increased expression of certain activated MAP Kinase signaling intermediates in T-BMDC is consistent with a recent report showing involvement of Erk MAP kinase in ER stress in human neuroblastoma cells (46). Notably, Hayakawa et al. (30) recently found that ER stress depresses NF-κB activation, which is in consort with our finding of diminished levels activated NF-κB intermediates in T-BMDC. These findings are also consistent with the observation by Zeyda et al. (2) who reported that exogenous administration of polyunsaturated fatty-acids PUFA lessened DC immune-stimulatory capacity independent of NF-κB signaling. However, our findings of enhanced Akt activation are surprising in this context since ER stress has been reported to negatively regulate the Akt/mTOR pathway (47). Further, PPAR-γ can also negatively regulate Akt phosphorylation (48). These data suggest that alternate mechanisms may be responsible for the elevated levels of pAkt in T-BMDC. It is also notable that MAP Kinase inhibition but not PI3K/Akt signaling blockade mitigated the enhanced T cell immune-stimulatory capacity of T-BMDC. Our data also imply that, besides their elevated ER stress and increased inflammatory pathway signaling, the enhanced effector cell stimulatory capacity of T-BMDC may be a function of their augmented cytokine secretory profile. DC production of varied cytokine has well established potent effects on their antigen presenting and allostimulaotry capacity (49).

Our study on the effects of endogenous fatty- acid synthesis inhibition on DC function expands on previous reports showing that exogenous administration of polyunsaturated fatty acids results in diminished TNF-α production, CD40 expression, and T cell stimulatory capacity in developing human moDC (2). However, taken in the context of our recent work, there appears to be a dichotomy between the effects of fatty-acid synthesis inhibition on DC developing from cellular precursors versus blockade of fatty-acid synthesis on fully mature DC populations. In particular, we recently reported that fully mature liver DC can be divided

into two distinct populations based on intracellular lipid content - including triglycerides and phospholipids (11). Further, we found that liver DC immunogenicity is determined by their lipid content, as lipid-rich liver DC were more immunogenic in comparison with lipid-poor liver DC. This was demonstrated by their higher secretion of cytokines and activation of antigen restricted $CD4^+$ and $CD8^+$ T cells as well as NK cells and NKT cells. Moreover, blockade of fatty-acid synthesis in terminally-differentiated lipid-rich liver DC using TOFA diminished their capacity for T cell and NK cell activation (11). Therefore, the effects of fatty-acids - or blockade of their production - on DC properties in the current study appears to be limited to developmental effects rather than applicable to mature fully-differentiated DC.

Supplementary Material

Refer to Web version on PubMed Central for supplementary material.

Acknowledgments

Grant Support: This work was supported in-part by National Institute of Health Awards DK085278 (GM) and CA155649 (GM).

References

1. Steinman RM, Banchereau J. Taking dendritic cells into medicine. Nature. 2007; 449:419–426. [PubMed: 17898760]
2. Zeyda M, Saemann MD, Stuhlmeier KM, Mascher DG, Nowotny PN, Zlabinger GJ, Waldhausl W, Stulnig TM. Polyunsaturated fatty acids block dendritic cell activation and function independently of NF-kappaB activation. J Biol Chem. 2005; 280:14293–14301. [PubMed: 15684433]
3. Herber DL, Cao W, Nefedova Y, Novitskiy SV, Nagaraj S, Tyurin VA, Corzo A, Cho HI, Celis E, Lennox B, Knight SC, Padhya T, McCaffrey TV, McCaffrey JC, Antonia S, Fishman M, Ferris RL, Kagan VE, Gabrilovich DI. Lipid accumulation and dendritic cell dysfunction in cancer. Nat Med. 2010; 16:880–886. [PubMed: 20622859]
4. Miller G, Lahrs S, Pillarisetty VG, Shah AB, DeMatteo RP. Adenovirus infection enhances dendritic cell immunostimulatory properties and induces natural killer and T-cell-mediated tumor protection. Cancer Res. 2002; 62:5260–5266. [PubMed: 12234994]
5. Kapadia SB, Chisari FV. Hepatitis C virus RNA replication is regulated by host geranylgeranylation and fatty acids. P Natl Acad Sci USA. 2005; 102:2561–2566.
6. Zhou W, Han WF, Landree LE, Thupari JN, Pinn ML, Bililign T, Kim EK, Vadlamudi A, Medghalchi SM, El Meskini R, Ronnett GV, Townsend CA, Kuhajda FP. Fatty acid synthase inhibition activates AMP-activated protein kinase in SKOV3 human ovarian cancer cells. Cancer research. 2007; 67:2964–2971. [PubMed: 17409402]
7. Pizer ES, Thupari J, Han WF, Pinn ML, Chrest FJ, Frehywot GL, Townsend CA, Kuhajda FP. Malonyl-coenzyme-A is a potential mediator of cytotoxicity induced by fatty-acid synthase inhibition in human breast cancer cells and xenografts. Cancer research. 2000; 60:213–218. [PubMed: 10667561]
8. Kashkar H, Kronke M, Jurgensmeier JM. Defective Bax activation in Hodgkin B-cell lines confers resistance to staurosporine-induced apoptosis. Cell Death Differ. 2002; 9:750–757. [PubMed: 12058280]
9. Belmokhtar CA, Hillion J, Segal-Bendirdjian E. Staurosporine induces apoptosis through both caspase-dependent and caspase-independent mechanisms. Oncogene. 2001; 20:3354–3362. [PubMed: 11423986]
10. Connolly MK, Bedrosian AS, Mallen-St Clair J, Mitchell AP, Ibrahim J, Stroud A, Pachter HL, Bar-Sagi D, Frey AB, Miller G. In liver fibrosis, dendritic cells govern hepatic inflammation in mice via TNF-alpha. J Clin Invest. 2009; 119:3213–3225. [PubMed: 19855130]

11. Ibrahim J, Nguyen AH, Rehman A, Ochi A, Jamal M, Graffeo CS, Henning JR, Zambirinis CP, Fallon N, Barilla R, Badar S, Mitchell A, Rao R, Acehan D, Frey AB, Miller G. Dendritic Cell Populations with Different Concentrations of Lipid Regulate Tolerance and Immunity in Mouse and Human Liver. Gastroenterology. 2012
12. Bedrosian AS, Nguyen AH, Hackman M, Connolly MK, Malhotra A, Ibrahim J, Cieza-Rubio NE, Henning JR, Barilla R, Rehman A, Pachter HL, Medina-Zea MV, Cohen SM, Frey AB, Acehan D, Miller G. Dendritic cells promote pancreatic viability in mice with acute pancreatitis. Gastroenterology. 2011; 141:1915–1926. e1911–1914. [PubMed: 21801698]
13. Landree LE, Hanlon AL, Strong DW, Rumbaugh G, Miller IM, Thupari JN, Connolly EC, Huganir RL, Richardson C, Witters LA, Kuhajda FP, Ronnett GV. C75, a fatty acid synthase inhibitor, modulates AMP-activated protein kinase to alter neuronal energy metabolism. J Biol Chem. 2004; 279:3817–3827. [PubMed: 14615481]
14. Thupari JN, Landree LE, Ronnett GV, Kuhajda FP. C75 increases peripheral energy utilization and fatty acid oxidation in diet-induced obesity. Proc Natl Acad Sci U S A. 2002; 99:9498–9502. [PubMed: 12060712]
15. Guseva NV, Rokhlin OW, Glover RA, Cohen MB. TOFA (5-tetradecyl-oxy-2-furoic acid) reduces fatty acid synthesis, inhibits expression of AR, neuropilin-1 and Mcl-1 and kills prostate cancer cells independent of p53 status. Cancer Biol Ther. 2011; 12:80–85. [PubMed: 21525791]
16. Wang C, Xu C, Sun M, Luo D, Liao DF, Cao D. Acetyl-CoA carboxylase-alpha inhibitor TOFA induces human cancer cell apoptosis. Biochem Biophys Res Commun. 2009; 385:302–306. [PubMed: 19450551]
17. Castilho G, Okuda LS, Pinto RS, Iborra RT, Nakandakare ER, Santos CX, Laurindo FR, Passarelli M. ER stress is associated with reduced ABCA-1 protein levels in macrophages treated with advanced glycated albumin - Reversal by a chemical chaperone. Int J Biochem Cell Biol. 2012
18. Abbas W, Khan KA, Tripathy MK, Dichamp I, Keita M, Rohr O, Herbein G. Inhibition of ER stress-mediated apoptosis in macrophages by nuclear-cytoplasmic relocalization of eEF1A by the HIV-1 Nef protein. Cell Death Dis. 2012; 3:e292. [PubMed: 22476100]
19. Seimon TA, Kim MJ, Blumenthal A, Koo J, Ehrt S, Wainwright H, Bekker LG, Kaplan G, Nathan C, Tabas I, Russell DG. Induction of ER stress in macrophages of tuberculosis granulomas. PLoS One. 2010; 5:e12772. [PubMed: 20856677]
20. Little JL, Wheeler FB, Fels DR, Koumenis C, Kridel SJ. Inhibition of fatty acid synthase induces endoplasmic reticulum stress in tumor cells. Cancer Res. 2007; 67:1262–1269. [PubMed: 17283163]
21. Wu Y, Zhang H, Dong Y, Park YM, Ip C. Endoplasmic reticulum stress signal mediators are targets of selenium action. Cancer Res. 2005; 65:9073–9079. [PubMed: 16204082]
22. Han KL, Choi JS, Lee JY, Song J, Joe MK, Jung MH, Hwang JK. Therapeutic potential of peroxisome proliferators--activated receptor-alpha/gamma dual agonist with alleviation of endoplasmic reticulum stress for the treatment of diabetes. Diabetes. 2008; 57:737–745. [PubMed: 18065517]
23. Weber SM, Chambers KT, Bensch KG, Scarim AL, Corbett JA. PPARgamma ligands induce ER stress in pancreatic beta-cells: ER stress activation results in attenuation of cytokine signaling. Am J Physiol Endocrinol Metab. 2004; 287:E1171–1177. [PubMed: 15315910]
24. Zapata-Gonzalez F, Rueda F, Petriz J, Domingo P, Villarroya F, Diaz-Delfin J, de Madariaga MA, Domingo JC. Human dendritic cell activities are modulated by the omega-3 fatty acid, docosahexaenoic acid, mainly through PPAR(gamma):RXR heterodimers: comparison with other polyunsaturated fatty acids. J Leukoc Biol. 2008; 84:1172–1182. [PubMed: 18632990]
25. Appel S, Mirakaj V, Bringmann A, Weck MM, Grunebach F, Brossart P. PPAR-gamma agonists inhibit toll-like receptor-mediated activation of dendritic cells via the MAP kinase and NF-kappaB pathways. Blood. 2005; 106:3888–3894. [PubMed: 16105976]
26. Palucka K, Banchereau J, Mellman I. Designing vaccines based on biology of human dendritic cell subsets. Immunity. 2010; 33:464–478. [PubMed: 21029958]
27. Pajtasz-Piasecka E, Indrova M. Dendritic cell-based vaccines for the therapy of experimental tumors. Immunotherapy. 2010; 2:257–268. [PubMed: 20635932]

28. Frankenberger B, Schendel DJ. Third generation dendritic cell vaccines for tumor immunotherapy. Eur J Cell Biol. 2012; 91:53–58. [PubMed: 21439674]
29. Watts C, West MA, Zaru R. TLR signalling regulated antigen presentation in dendritic cells. Curr Opin Immunol. 2010; 22:124–130. [PubMed: 20083398]
30. Hayakawa K, Nakajima S, Hiramatsu N, Okamura M, Huang T, Saito Y, Tagawa Y, Tamai M, Takahashi S, Yao J, Kitamura M. ER stress depresses NF-kappaB activation in mesangial cells through preferential induction of C/EBP beta. J Am Soc Nephrol. 2010; 21:73–81. [PubMed: 19875812]
31. Granados DP, Tanguay PL, Hardy MP, Caron E, de Verteuil D, Meloche S, Perreault C. ER stress affects processing of MHC class I-associated peptides. BMC Immunol. 2009; 10:10. [PubMed: 19220912]
32. Basseri S, Lhotak S, Sharma AM, Austin RC. The chemical chaperone 4-phenylbutyrate inhibits adipogenesis by modulating the unfolded protein response. J Lipid Res. 2009; 50:2486–2501. [PubMed: 19461119]
33. Miller G, Lahrs S, Dematteo RP. Overexpression of interleukin-12 enables dendritic cells to activate NK cells and confer systemic antitumor immunity. Faseb J. 2003; 17:728–730. [PubMed: 12594171]
34. Chan CW, Crafton E, Fan HN, Flook J, Yoshimura K, Skarica M, Brockstedt D, Dubensky TW, Stins MF, Lanier LL, Pardoll DM, Housseau F. Interferon-producing killer dendritic cells provide a link between innate and adaptive immunity. Nat Med. 2006; 12:207–213. [PubMed: 16444266]
35. Kijima M, Yamaguchi T, Ishifune C, Maekawa Y, Koyanagi A, Yagita H, Chiba S, Kishihara K, Shimada M, Yasutomo K. Dendritic cell-mediated NK cell activation is controlled by Jagged2-Notch interaction. Proc Natl Acad Sci U S A. 2008; 105:7010–7015. [PubMed: 18458347]
36. Zhou W, Simpson PJ, McFadden JM, Townsend CA, Medghalchi SM, Vadlamudi A, Pinn ML, Ronnett GV, Kuhajda FP. Fatty acid synthase inhibition triggers apoptosis during S phase in human cancer cells. Cancer Res. 2003; 63:7330–7337. [PubMed: 14612531]
37. Makela SM, Strengell M, Pietila TE, Osterlund P, Julkunen I. Multiple signaling pathways contribute to synergistic TLR ligand-dependent cytokine gene expression in human monocyte-derived macrophages and dendritic cells. J Leukoc Biol. 2009; 85:664–672. [PubMed: 19164128]
38. Caparros E, Munoz P, Sierra-Filardi E, Serrano-Gomez D, Puig-Kroger A, Rodriguez-Fernandez JL, Mellado M, Sancho J, Zubiaur M, Corbi AL. DC-SIGN ligation on dendritic cells results in ERK and PI3K activation and modulates cytokine production. Blood. 2006; 107:3950–3958. [PubMed: 16434485]
39. Rice CM, Scolding NJ. Adult human mesenchymal cells proliferate and migrate in response to chemokines expressed in demyelination. Cell Adh Migr. 2010; 4:235–240. [PubMed: 20234187]
40. Stober D, Schirmbeck R, Reimann J. IL-12/IL-18-dependent IFN-gamma release by murine dendritic cells. Journal of immunology. 2001; 167:957–965.
41. Ueno H, Klechevsky E, Schmitt N, Ni L, Flamar AL, Zurawski S, Zurawski G, Palucka K, Banchereau J, Oh S. Targeting human dendritic cell subsets for improved vaccines. Semin Immunol. 2011; 23:21–27. [PubMed: 21277223]
42. Hetz C. The unfolded protein response: controlling cell fate decisions under ER stress and beyond. Nat Rev Mol Cell Biol. 2012; 13:89–102. [PubMed: 22251901]
43. Wu J, Kaufman RJ. From acute ER stress to physiological roles of the Unfolded Protein Response. Cell Death Differ. 2006; 13:374–384. [PubMed: 16397578]
44. Goodall JC, Wu C, Zhang Y, McNeill L, Ellis L, Saudek V, Gaston JS. Endoplasmic reticulum stress-induced transcription factor, CHOP, is crucial for dendritic cell IL-23 expression. Proc Natl Acad Sci U S A. 2010; 107:17698–17703. [PubMed: 20876114]
45. Oh J, Riek AE, Weng S, Petty M, Kim D, Colonna M, Cella M, Bernal-Mizrachi C. Endoplasmic reticulum stress controls M2 macrophage differentiation and foam cell formation. J Biol Chem. 2012; 287:11629–11641. [PubMed: 22356914]
46. Arai K, Lee SR, van Leyen K, Kurose H, Lo EH. Involvement of ERK MAP kinase in endoplasmic reticulum stress in SH-SY5Y human neuroblastoma cells. J Neurochem. 2004; 89:232–239. [PubMed: 15030407]

47. Qin L, Wang Z, Tao L, Wang Y. ER stress negatively regulates AKT/TSC/mTOR pathway to enhance autophagy. Autophagy. 2010; 6:239–247. [PubMed: 20104019]

48. Goetze S, Eilers F, Bungenstock A, Kintscher U, Stawowy P, Blaschke F, Graf K, Law RE, Fleck E, Grafe M. PPAR activators inhibit endothelial cell migration by targeting Akt. Biochem Biophys Res Commun. 2002; 293:1431–1437. [PubMed: 12054675]

49. Morelli AE, Zahorchak AF, Larregina AT, Colvin BL, Logar AJ, Takayama T, Falo LD, Thomson AW. Cytokine production by mouse myeloid dendritic cells in relation to differentiation and terminal maturation induced by lipopolysaccharide or CD40 ligation. Blood. 2001; 98:1512–1523. [PubMed: 11520802]

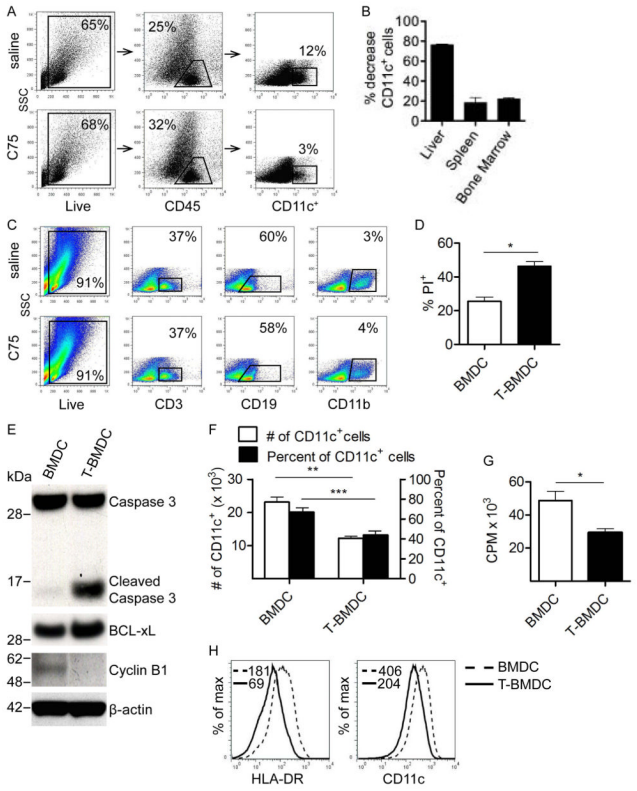

Figure 1. Blockade of fatty-acid synthesis inhibits dendropoiesis in mice and humans

(a–c) Mice were treated for four weeks with C75 or saline. **(a)** Live CD45$^+$ liver leukocytes were gated using flow cytometry and the sub-fraction of hepatic CD11c$^+$ cells was determined. **(b)** The percentage decrease in the number of liver, spleen, and bone marrow DC was calculated. **(c)** The fraction of splenocytes expressing CD3, CD19, and CD11b in saline- or C75-treated mice was tested. **(d–g)** BMDC were grown alone or with TOFA. **(d)** The fraction of PI$^+$ cells was calculated on day 8 of culture. **(e)** Day 8 BMDC and T-BMDC were also tested for expression of Caspase 3, Cleaved Caspase 3, BCL-xL, Cyclin B1, and β-actin by Western blotting. **(f)** In addition, the total number and fraction of CD11c$^+$ cells was calculated in day 8 BMDC and T-BMDC cultures. **(g)** Cellular proliferation was compared in day 8 BMDC and T-BMDC by pulsing with 3H-Thymidine. **(h)** moDC grown in control media and TOFA-enriched media were tested for HLA-DR and CD11c expression. Median fluorescence index (MFI) is indicated for each respective histogram (*p<0.05; **p<0.01; ***p<0.001).

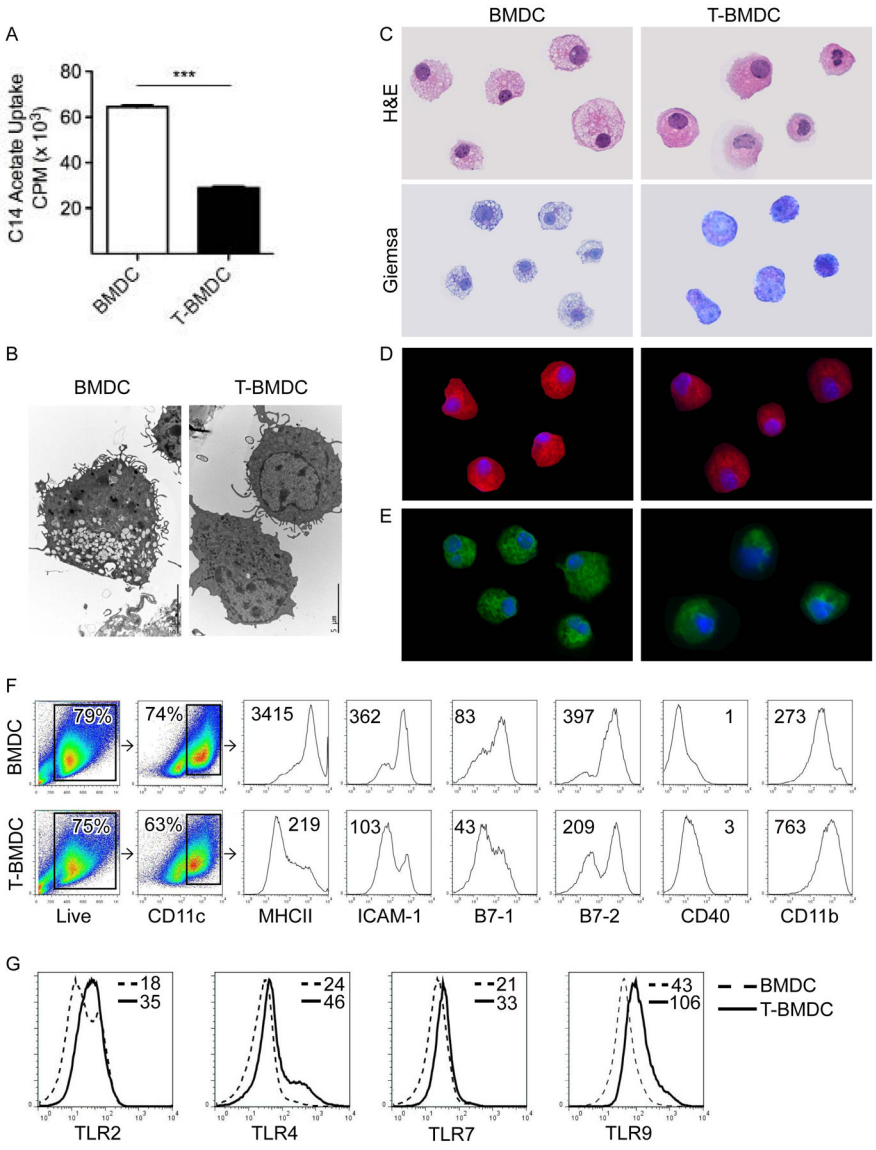

Figure 2. Blockade of fatty-acid synthesis alters DC phenotype

(a) C-14 acetate uptake was compared in day 8 BMDC and T-BMDC cultures (***p<0.001). **(b–e)** Day 8 BMDC and T-BMDC were examined by **(b)** electron microscopy, **(c)** H&E and Gimsea staining, or **(d)** immunofluorescence using HCS LipidTOX Red which binds neutral lipids and **(e)** HCS LipidTOX Green which binds phospholipids. **(f)** $CD11c^{+}$ cells in BMDC or T-BMDC cultures were gated and analyzed for expression of MHCII, adhesion, and co-stimulatory molecules as well as **(g)** TLR2, TLR4, TLR7, and TLR9. MFIs are indicated for each respective histogram.

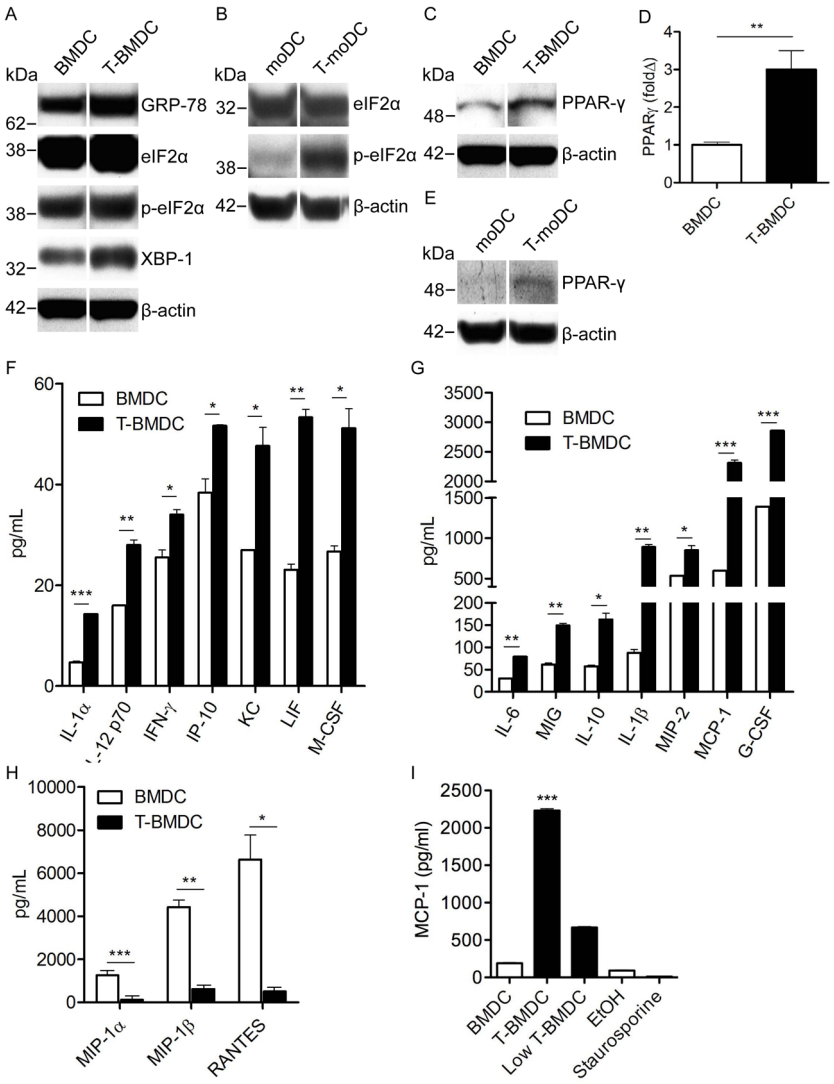

Figure 3. Inhibition of fatty-acid synthesis during DC development increases ER stress and alters DC production of inflammatory mediators

(a) Expression of markers of ER stress (GRP-78, eIF2α, p- eIF2α, XBP-1) was tested in day 8 BMDC and T-BMDC by Western blotting. **(b)** Human moDC generated in control or TOFA-enriched media were tested for expression of selected ER stress markers. **(c)** Control or TOFA-treated murine BMDC were tested for expression of PPAR-γ by Western blotting and **(d)** PCR. **(e)** Human moDC generated in control media or TOFA-supplemented media were tested for expression of PPAR-γ by Western blotting. β-actin was used as a loading control. **(f–h)** 24 hour cell culture supernatants from day 8 BMDC and T-BMDC plated at equal densities were tested for the presence of numerous cytokines and chemokines. **(i)** Control BMDC, high-dose TOFA-treated BMDC, standard low-dose TOFA-treated BMDC, ethanol-trreated BMDC, and staurosporine-treated BMDC were tested for their capacity to produce MCP-1 (*p<0.05; **p<0.01; ***p<0.001).

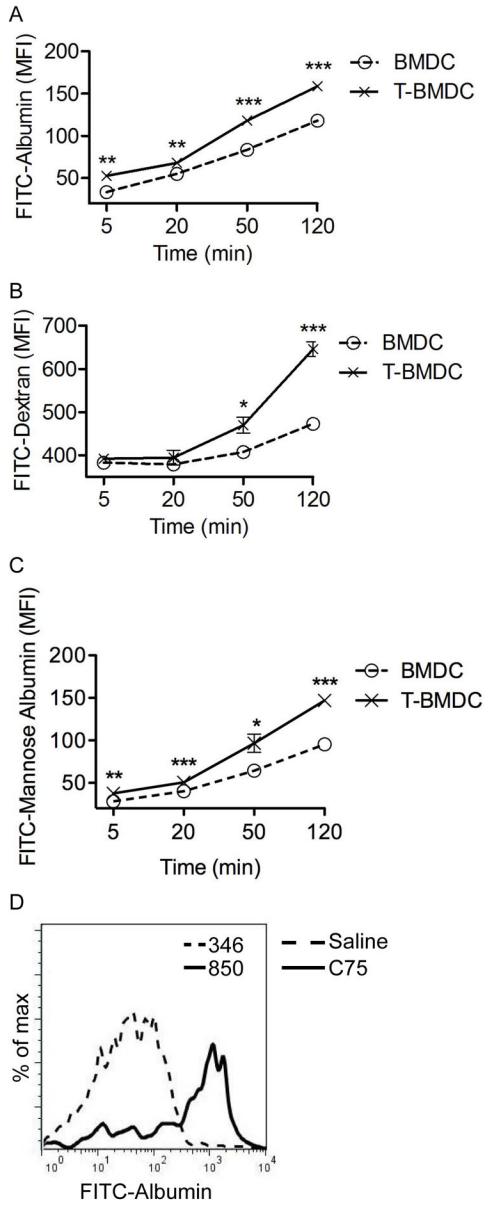

Figure 4. Blockade of fatty-acid synthesis enhances DC capacity for antigen capture in vitro and in vivo

(a–c) BMDC and T-BMDC were tested at various time points for uptake of fluorescent **(a)** Albumin, **(b)** Dextran, and **(c)** Mannosylated Albumin (*p<0.05; **p<0.01; ***p<0.001). **(d)** Splenic $CD11c^{+}$ cells from control or C75 treated mice were tested for uptake of FITC-Albumin at 30 minutes after in vivo administration. Data are representative of experiments performed 3 times.

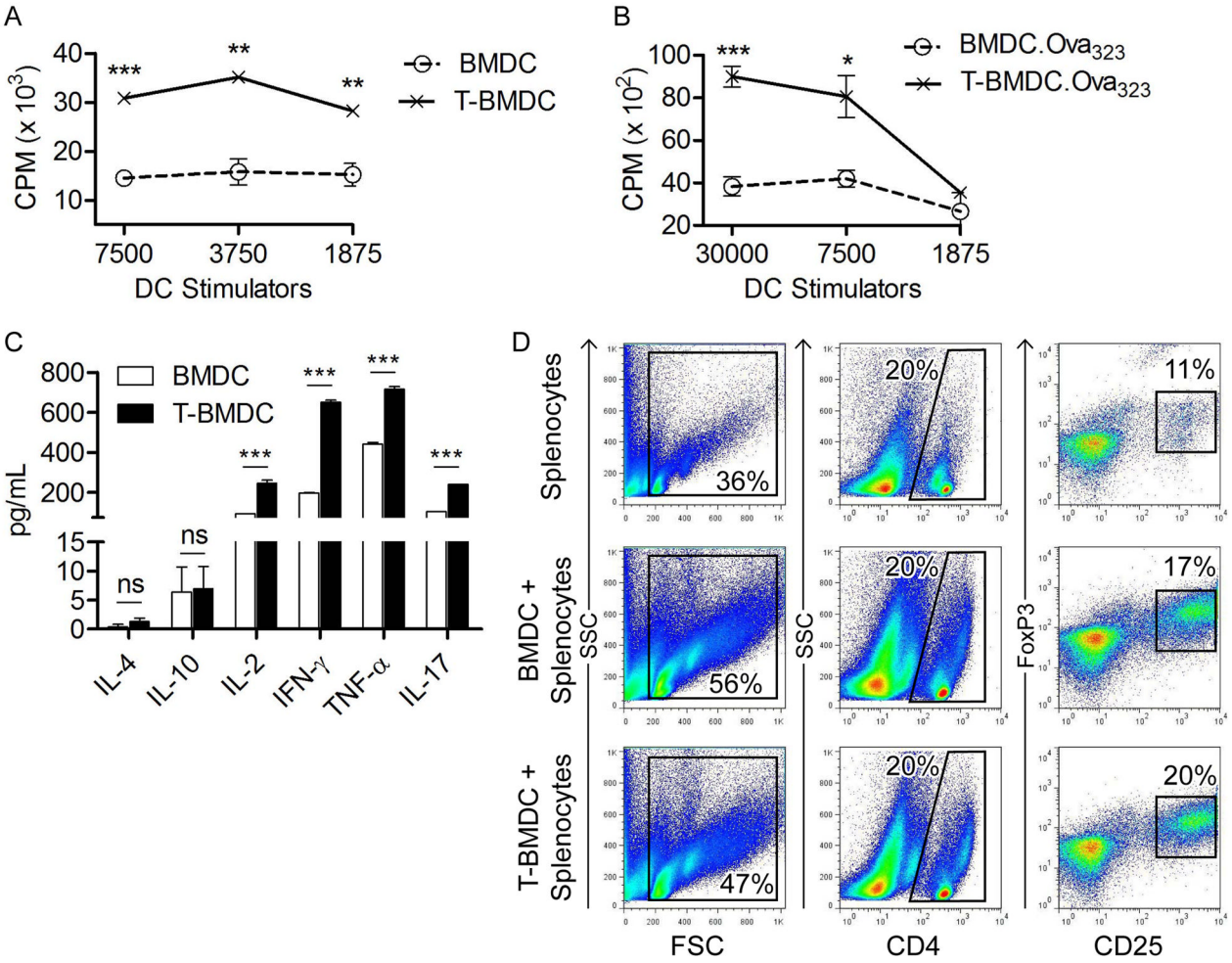

Figure 5. T-BMDC induce enhanced allogeneic and antigen-restricted CD4$^+$ T cell stimulation

(a) Various concentrations of BMDC and T-BMDC were tested for their ability to induce proliferation of allogeneic T cells in an MLR. **(b, c)** BMDC and T-BMDC pulsed with $Ova_{323–339}$ peptide were tested for their ability to induce **(b)** antigen-restricted CD4$^+$ T cell proliferation and **(c)** Th1, Th2, and Th17 cytokine production in OT-II T cells (*p<0.05; **p<0.01; ***p<0.001). **(d)** CD4$^+$ T cell co-expression of CD25 and FoxP3 was tested at 96 hours after splenocytes were co-cultured in a 1:1 ratio with BMDC or T-BMDC.

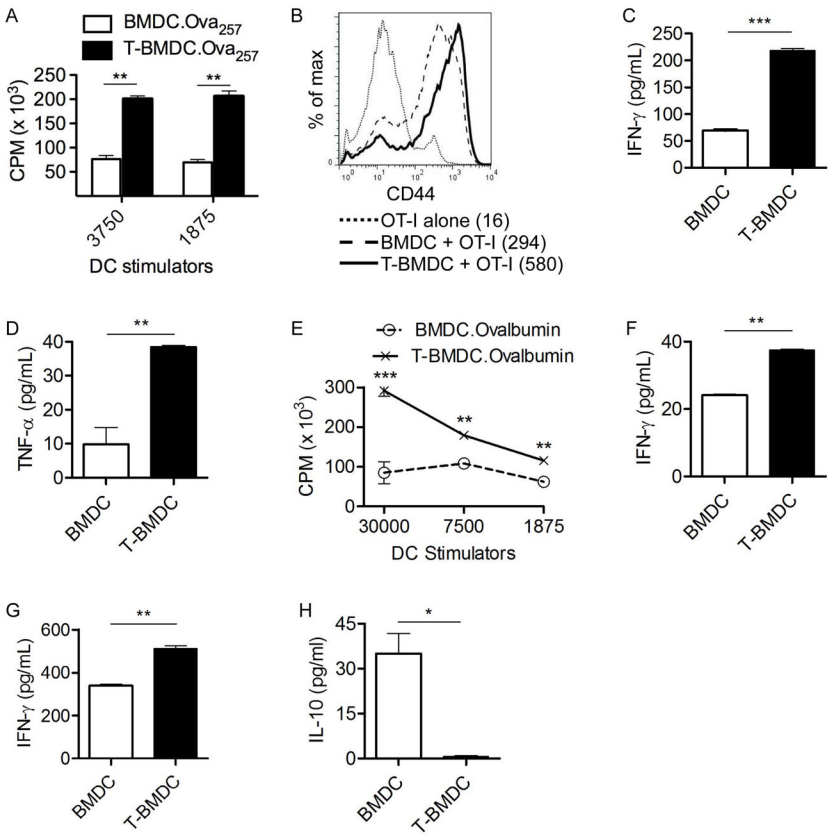

Figure 6. T-BMDC induce enhanced CD8$^+$ T cell activation

(a–d) BMDC and T-BMDC were loaded with $Ova_{257–264}$ peptide and plated in various ratios with CD8$^+$ OT-I T cells. **(a)** OT-I proliferation was measured by incorporation of 3H-Thymidine. **(b)** OT-I T cell expression of CD44 was measured on flow cytometry (MFI is indicated). **(c)** IFN-γ and **(d)** TNF-α production by CD8$^+$ OT-I T cells was measured in cell culture supernatant. **(e, f)** To test DC capacity for cross-presentation, BMDC and T-BMDC were loaded with Ovalbumin and used in various ratios to stimulate CD8$^+$ OT-I T cells. **(e)** OT-I cellular proliferation and **(f)** production of IFN-γ were measured. **(g, h)** Restimulated CTL cultures from mice twice-immunized by adoptive transfer of $Ova_{257–264}$ peptide-pulsed BMDC or T-BMDC were tested for production of **(g)** IFN-γ and **(h)** IL-10 (*p<0.05; **p<0.01; ***p<0.001).

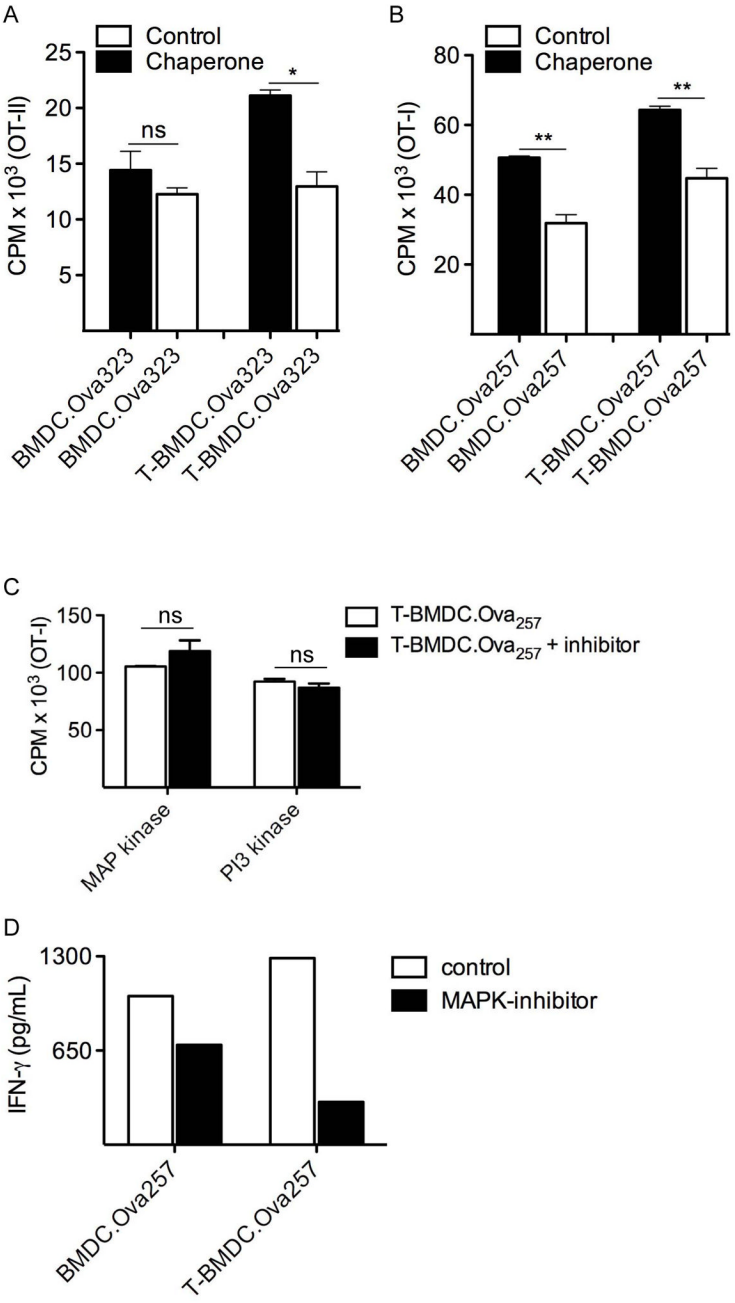

Figure 7. Lowering ER stress reduces the enhanced T cell stimulatory capacity of T-BMDC

(a, b) BMDC or T-BMDC (1×10^4) were loaded with the appropriate Ova peptide and used to stimulate **(a)** $CD4^+$ OT-II T cells or **(b)** $CD8^+$ OT-I T cells, respectively, for 72h. In selected experiments, DC were pre-incubated with the chaperone 4-phenylbutyrate (*$p<0.05$; **$p<0.01$). **(c)** OTI-I T cell stimulation assays were repeated using soluble PI3 Kinase and MAP Kinase inhibitors. T cell proliferation was measured by incorporation of 3H-Thymidine during the last 24h. **(d)** OT-I T cell activation after stimulation by peptide-pulsed BMDC in the context of MAP kinase inhibition or control was measured by production of IFN-γ. Representative data is shown from experiments repeated three times.

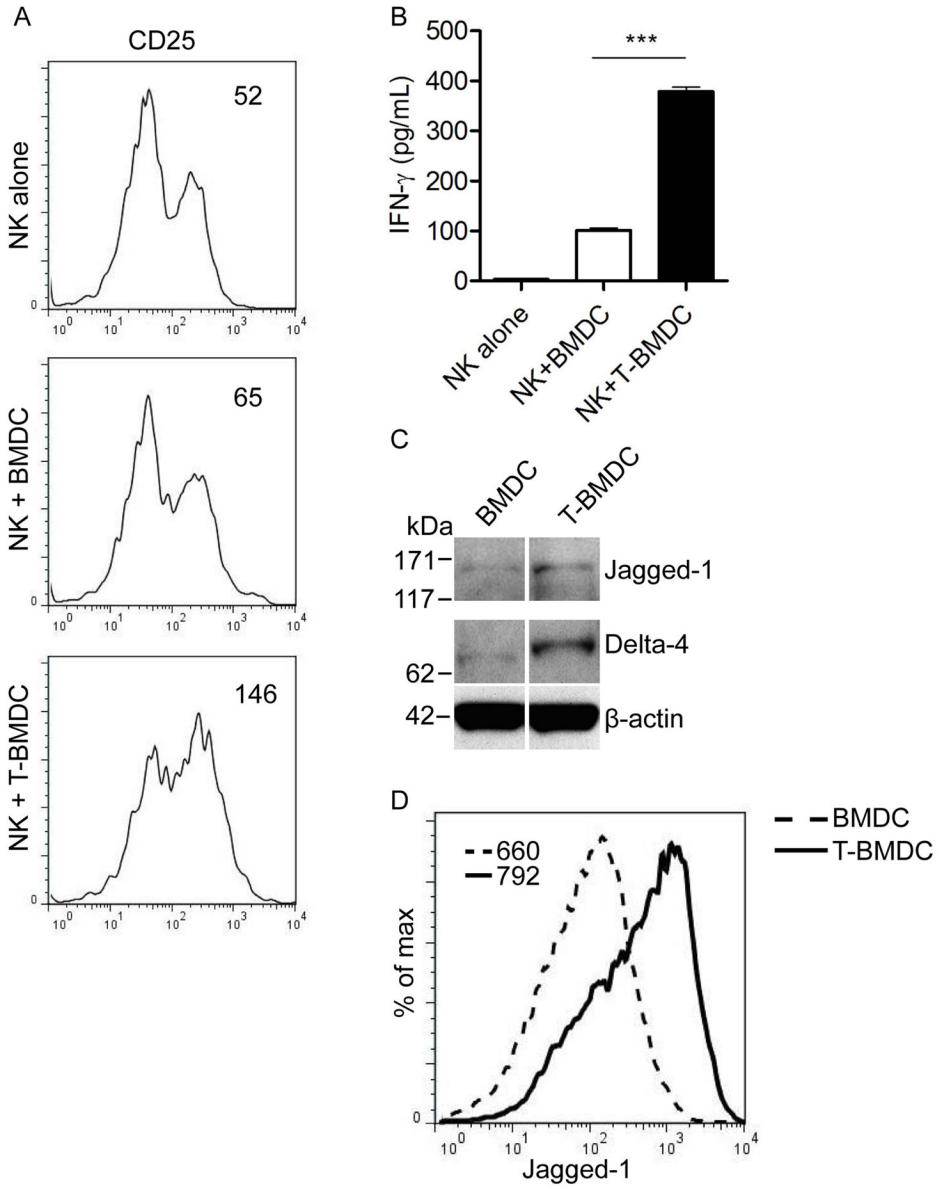

Figure 8. T-BMDC have enhanced capacity for NK cell activation

(a–d) Spleen NK cells were harvested and co-incubated with BMDC or T-BMDC. NK cell **(a)** expression of CD25 (MFI is indicated), **(b)** production of IFN-γ (***p<0.001), **(c, d)** and expression of Notch ligands were measured by **(c)** Western blotting (Jagged-1, Delta-4) and **(d)** flow cytometry (Jagged-1).